Original Research

C. Stumpp*
W. Stichler
M. Kandolf
J. Šimůnek

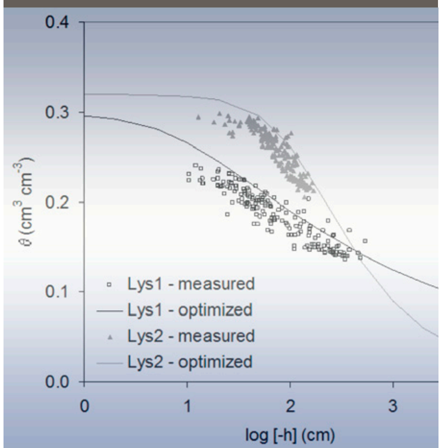

We investigated differences in water flow and solute transport due to different land use in five long-term lysimeter studies. Stable water isotopes were key parameters providing insight into mean transit times and effective water contents. Both land use and nonuniform infiltration patterns during snow melt impacted water flow and solute transport.

C. Stumpp and J. Šimůnek, Dep. of Environmental Sciences, Univ. of California, Riverside, CA 92521, USA; C. Stumpp and W. Stichler, Helmholtz Zentrum München–German Research Center for Environmental Health–Institute of Groundwater Ecology, Ingolstädter Landstr. 1, D-85764 Neuherberg, Germany; M. Kandolf, Höhere Bundeslehr- und Forschungsanstalt für Landwirtschaft (HBLFA) Raumberg-Gumpenstein, Abteilung für Umweltökologie, Raumberg 38, A-8952 Irdning, Austria. *Corresponding author (christine.stumpp@helmholtz-muenchen.de).

Vadose Zone J.
doi:10.2136/vzj2011.0075
Received 27 June 2011.

Effects of Land Cover and Fertilization Method on Water Flow and Solute Transport in Five Lysimeters: A Long-Term Study Using Stable Water Isotopes

Land cover and agricultural management practices can significantly influence soil structure. However, little is known about how fertilizer applications and land cover affect soil hydrology and groundwater recharge over long time periods. The objective of this study was to use stable water isotopes as environmental tracers to provide additional information required for better understanding of water flow and solute transport processes in the unsaturated zone influenced by land cover and type of fertilizer applications. Five lysimeters containing undisturbed soil monoliths from the same agricultural field site were investigated over a period of 5 yr. Liquid cattle slurry and solid animal manure were applied to the maize (*Zea mays* L.) and winter rye (*Secale cereale* L.) lysimeters. The grass–clover lysimeter was treated with mineral fertilizer. Quantitative influence of land cover and type of fertilizer application on water flow and solute transport was evaluated for all lysimeters using a modified version of HYDRUS-1D. The highest drainage was observed in the maize lysimeter treated with cattle slurry, and the lowest in the grass lysimeter treated with mineral fertilizer. Pronounced differences in water contents and estimated saturated hydraulic conductivities between the lysimeters were restricted to the upper 25 to 30 cm of the soil. In particular, the lysimeters treated with animal manure had higher porosities, indicating a higher content of organic matter. Main differences in discharge between the lysimeters were observed in spring and during the plant growth periods, indicating the importance of nonuniform, patchy infiltration patterns during snow melt and of root water uptake, respectively. Mean water flow velocities, transit times, and effective water contents were estimated from the stable water isotope data, providing evidence on the impact of land cover and type of fertilizer application. We found smaller mean transit times in the maize lysimeters and for soils with liquid cattle slurry applications. Simulations indicate that numerical modeling can reproduce the general trend of water flow and isotope transport. Despite differences in mean transit times, fitted dispersivities were all in the same range, suggesting similar soil structures in the five lysimeters. However, more data for calibration and more information about heterogeneous infiltration would be required to improve the model accuracy. In general, stable water isotopes clearly contributed an added value, elucidating differences in mean flow parameters between the lysimeters. Thus, they provided evidence of the impacts of land cover and fertilizer applications, which are not obvious from water balance and mean discharge rates alone.

Abbreviations: BCs, boundary conditions; LAI, leaf area index; LMWL, local meteoric water line; Lys, lysimeter; NSE, Nash–Sutcliffe efficiency; TDR, time domain reflectometry; V-SMOW, Vienna-Standard Mean Ocean Water.

Soil hydraulic properties control infiltration and movement of water and solutes through the unsaturated zone. Particularly in agricultural soils, knowledge of these properties is essential to predict water fluxes affecting the crop yield and the fate of agrochemicals affecting the groundwater quality. Numerous studies have shown that soil hydraulic properties, bulk density, and soil structure are affected by land use and agricultural management practices (Coutadeur et al., 2002; Miller et al., 2002; Bormann and Klaassen, 2008; Fares et al., 2008; Bachmair et al., 2009; Hu et al., 2009; Chakraborty et al., 2010). Cultivated soils are exposed to continual changes and ongoing soil structural development due to plowing, addition of fertilizers, and plant and root growth. These changes can result in the development of different pore-size distributions in the same initial soil material and can induce spatial variations in water flow and solute transport. A summary of various effects on soil properties, focusing mainly on wheel track compaction, tillage, and macropore systems, was given by Green et al. (2003). Schwartz et al. (2003) showed that land use (native grassland, recently tilled cropland, and re-established grassland) influenced the pore structure and bulk density in the upper 20 cm of the soil profile. In the study, differences in soil hydraulic properties were impacted more by the type of vegetation than by the type of soil. Although topsoil properties, such as bulk density and organic matter content, were influenced by different land use in four soil series, different times when hydraulic conductivities were measured (either in spring or autumn) produced more variable results than the soil type and land use (Zhou et al., 2008). However, whether these temporal variations could be explained by hysteresis effects remains unknown. Ndiaye et al. (2007) compared the influence of two agricultural practices on soil hydraulic properties. They used mineral fertilizer for maize plots and pig slurry for a grass–maize rotation and found a one order of magnitude difference in hydraulic conductivities in the upper 35 cm. Bachmair et al. (2009) qualitatively investigated water flow at five sites with similar texture, different land cover (grass, farmland, forest), and land use (tilled and untilled). Preferential flow, which was observed at all sites, differed according to soil structure, microtopography, texture, and soil cover. An increase in the infiltration rate was not always accompanied by an increase in preferential flow. Flow conditions were highly complex and variable, highlighting the importance of structural heterogeneities and spatial variability.

As indicated above, most studies have evaluated how various factors affected soil hydraulic properties near the soil surface or leaching of nutrients (Knappe et al., 2002; van Es et al., 2004, 2006). However, little is known about their indirect influence on water flow, groundwater recharge, and solute transport. The question remains whether these changes near the soil surface, resulting from different fertilizer applications or land cover, have any net effect on groundwater recharge over long time periods or whether they merely impact soil structure. Particularly for highly vulnerable agricultural soils, we need to understand the influence of fertilization methods and the growth of different plants, not only on the development of soil structure and soil hydraulic properties, but also on water flow and solute transport. Knowledge of spatial heterogeneities is required for the adequate use of mathematical models (Herbst et al., 2005; Stumpp et al., 2009b), the design of effective irrigation systems (Green et al., 2006), and predictions on whether nutrients (Kosmas et al., 1991), pesticides (Pot et al., 2005; Stone and Wilson, 2006), or water may bypass the root zone as a result of preferential flow (Gärdenäs et al., 2006). Heterogeneities in real-world soils and their effects on soil–plant–atmosphere interactions have to be investigated so that the upscaling of crucial processes can finally be fully understood for more than just bare soils (Vereecken et al., 2007).

As mentioned above, structural heterogeneities, such as changes of soil due to vegetation and treatment, can result in water flux heterogeneities and/or preferential flow. Other water flux heterogeneities are induced by patchy infiltration patterns and water content distributions within the soil profile due to vegetation (e.g., Oswald et al., 2008), snow melt/frozen soil (Bayard et al., 2005), or differences in surface slopes (Bergkamp, 1998).

Lysimeters, combined with the use of stable isotopes and mathematical modeling, are adequate experimental tools for obtaining valuable information about the impact of fertilization method and land cover on water flow at the scale of agricultural fields. Lysimeters, containing undisturbed, cultivated soils, are exposed to natural environmental conditions, which can be measured in situ over time. Using several lysimeters, containing initially the same soil, can enable us to investigate soil hydrology as it is affected by fertilization method and land cover.

Lysimeters have been used successfully together with stable water isotopes as environmental tracers to identify flow heterogeneities in different sandy soils and to improve the applicability of both lumped-parameter and transient mechanistic flow and transport models in the unsaturated zone (Maciejewski et al., 2006; Maloszewski et al., 2006; Stumpp et al., 2009a,c). These studies showed that the ratios of water isotopes ($\delta^{18}O$ and $\delta^{2}H$) are ideal tracers for investigating flow processes in the unsaturated zone in both bare and planted sandy soils, under humid climatic conditions. On the contrary, single, artificial, one-time tracer injections (e.g., dye tracer experiments) can only reveal information for a specific point of time, and thus for specific initial and boundary conditions. Information about stable water isotopes in precipitation and lysimeter discharge provides an integral description about water flow and solute transport processes over time. Uniform flow, as well as preferential flow, can be quantified quite well using water isotopes (Stumpp et al., 2007; Stumpp and Maloszewski, 2010). For example, quantitative differences in preferential flow and in distributions of transit times, both due to land use, were found (Stumpp and Maloszewski, 2010). The greatest mean transit times (52 wk) were observed for lysimeters with maize, compared to those with mustard (*Brassica* L.) or grains (42 wk). On average, 3% of total precipitation contributed to preferential flow in the lysimeter with grains, which was more than in lysimeters with mustard (2.2%) or maize (1%). Water isotopes combined with a dual-continuum modeling approach were also successfully used as tracers to determine preferential flow paths on the hill slope scale (Vogel et al., 2010).

The objective of this study is to provide a comprehensive understanding of water flow in cultivated soils under natural conditions and whether fertilization methods and land cover affect soil hydrology and groundwater recharge over long time periods. Moreover, we investigate if stable water isotopes used as environmental tracers can provide additional information required for better understanding of soil hydrological processes. For that purpose, five lysimeters containing undisturbed soil monoliths from the same field site were investigated. The lysimeters were embedded in agricultural fields, which were planted with different crops and treated with different fertilization methods. Soil hydraulic properties, drainage water fluxes, and water isotope concentrations were measured to understand differences between three different land covers (maize, rye, and grass–clover) and three different fertilization treatments (liquid cattle slurry, solid animal manure, and commercial phosphorus–potassium fertilizer). The quantitative influence of land use on water flow and solute transport was evaluated for all lysimeters using a modified version of HYDRUS-1D (Šimůnek et al., 2008).

Experimental Setup

The experimental site is located at the research area of the HBLFA Raumberg-Gumpenstein (47°30′ N, 14°6′ E, 700 m elevation) in Gumpenstein, 190 km southwest of Vienna (Austria). It is a humid region, with a mean annual temperature of 6.9°C and a mean annual precipitation of 1035 mm.

Since 1999, five lysimeters (Lys1–Lys5) have been embedded in agricultural fields (8 by 2.5 m) that differed in their crop and fertilization methods (Stichler et al., 2005). Liquid cattle slurry (Lys1, Lys3) and solid animal manure (Lys2, Lys4) were applied to the maize (Lys1, Lys2) and winter rye fields (Lys3, Lys4). The fertilizers were applied on the soil surface and manually incorporated into the upper 20 cm of the soil during sowing times. The fertilizers were additionally sprayed on the maize lysimeters in June. Maize was sown annually at the beginning of May and harvested in September or October. Winter rye was sown each year in October and harvested between the end of August and the beginning of October. Additionally, a grass–clover mixture was planted at the fifth field (Lys5), which was fertilized with phosphorous–potassium mineral fertilizer in the spring. The grass–clover mixture was maintained using a three-cut system.

Cylindrical lysimeters contained undisturbed soil monoliths of Dystric Cambisol with three soil horizons (A_p: 0–25 cm, B_v: 26–100 cm, C_v: >100 cm). However, thicknesses of the soil horizons varied slightly between the lysimeters and were not individually identified during the installation. Lysimeter vessels were pushed into the soil without any disturbance and cut at the bottom (Eder and Stenitzer, 2003). A layer of fluvioglacial sediments (5 cm), acting as a capillary barrier and enabling seepage face boundary conditions for modeling, and a plate with tubes for free drainage were installed at the bottom. The lysimeters were placed in the agricultural fields at the same spots as originally collected. They had a depth of 1.5 m and a surface area of 1 m^2. The land surface had a slope of 5°. To allow manual cultivation, the upper 30 cm of the stainless-steel lysimeter vessels were removable. Time domain reflectometry (TDR) probes (Trase, UMS GmbH, Munich, Germany) measuring water contents were installed at seven depths (10, 15, 25, 45, 70, 100, and 130 cm), and the data were logged starting in 2004. At the end of the observation period in 2007, tensiometers measuring soil water pressure heads (T4 type, UMS GmbH, Munich, Germany) were installed in three depths (20, 40, and 100 cm). Apart from these in situ measured variables, texture was analyzed (sieving, sedimentation) and soil hydraulic properties $\theta(h)$ and $K(h)$ were determined in laboratory drainage experiments on 100-cm^3 soil samples, collected from four different depths close to the lysimeters during their installation in 1999.

Between May 2002 and February 2007, precipitation and seepage water from the lysimeters were collected on an event basis and in weekly intervals, respectively. Samples were analyzed for $\delta^{18}O$ and δ^2H contents using dual-inlet mass spectrometry (e.g., at the IAEA, Vienna, or at the HMGU, Institute of Groundwater Ecology, Neuherberg), having a precision of ±1‰ for ^2H and ±0.15‰ for ^{18}O. The content of isotopes (R_{sample}) is given in the delta notation as the δ-content (‰), which is a relative deviation from the standard ($R_{standard}$):

$$\delta\,[‰] = \frac{R_{Sample} - R_{Standard}}{R_{Standard}} 1000 \quad [1]$$

The Vienna-Standard Mean Ocean Water (V-SMOW) is the mean isotope content of seawater, and is used as a reference standard. Positive δ contents indicate enrichment relative to the standard; negative contents indicate depletion. More details about principles of isotope hydrology and measurement techniques are given by the IAEA (1983) and Leibundgut et al. (2009).

Meteorological parameters were measured at the research site, and used to calculate daily potential evapotranspiration (ET_o) using the Penman–Monteith equation (Penman, 1948; Monteith, 1965):

$$ET_0 = \frac{1}{\lambda} \frac{\Delta(R_n - G) + \rho c_p \frac{(e_s - e_a)}{r_a}}{\Delta + \gamma\left(1 + \frac{r_c}{r_a}\right)} \quad [2]$$

where ET_0 is the potential evapotranspiration [L T^{-1}], λ is the latent heat of vaporization [L^2 T^{-2}], Δ is the slope of the vapor pressure curve [M L^{-1} T^{-2} K^{-1}], R_n is net radiation [M T^{-3}], G is the soil heat flux density [M T^{-3}], ρ is the atmospheric density [M L^{-3}], c_p is the specific heat of the air [L^2 T^{-2} K^{-1}], e_s is the saturation vapor pressure [M L^{-1} T^{-2}], e_a is the actual vapor pressure [M L^{-1} T^{-2}], r_c is the crop canopy resistance [T L^{-1}], r_a is the aerodynamic resistance [T L^{-1}], and γ is the psychrometric constant [M L^{-1} T^{-2} K^{-1}]. The parameters r_a and r_c were calculated individually for each plant from the crop heights, leaf area index (LAI) and wind velocity measurements (Allen et al., 1998). Information about the leaf area index and plant growth were taken from Knisel and Davis (2000) and the FAO-56 guidelines (Allen, 2000). Unknown parameters about crops (maximum root length, maximum crop height, LAI) were estimated according to personal communications with onsite operators and the literature (Allen, 2000). Thus, the maximum root depth was set to 100 and 60 cm for crops and grass (Bohner et al., 2007), respectively, and the maximum crop height (maximum LAI) of 170 cm (2.85), 130 cm (2.85), and 50 cm (5.0) was assumed for maize, rye, and grass (also considering the three-cut system), respectively.

Estimation of Mean Transit Times and Flow Parameters

Although the amplitude of the seasonal signal of the isotope contents in precipitation is attenuated in the lysimeters due to dispersion, it is still observable in the discharge of the lysimeters. This enabled us to estimate mean transit times of water by looking at the convective shift in the isotope peaks between the input and output and considering dispersion effects. The most pronounced and distinct correspondence was found in all lysimeters between the depleted (i.e., more negative δ contents) precipitation peak of the winter period of 2005–2006 and its corresponding lysimeter discharge. During this time period (18 Nov. 2005 to 14 Apr. 2006), the isotope content in precipitation was smaller than its mean weighted value. Likewise, the time period containing this winter signal had smaller isotope contents in the discharge than its mean weighted value. The difference between the centers of these two time periods, t_q [T] and t_p [T], defines the estimated mean peak concentration time t^*_m [T]:

$$t_m^* = \left(\frac{t_{q1}+t_{q2}}{2}\right) - \left(\frac{t_{p1}+t_{p2}}{2}\right) = t_q - t_p \qquad [3]$$

where t_{p1} and t_{p2} are times [T] when the period with depleted isotopes from winter precipitation starts and ends (isotope contents are smaller than the weighted mean value), respectively, and t_{q1} and t_{q2} are corresponding times for isotopes in the discharge. Accounting for dispersion effects, the mean estimated transit time t^*_0 [T] can be determined according to (Leibundgut et al., 2009):

$$t_0^* = \frac{t_m^*}{\sqrt{1+\left(3\frac{\lambda_L}{L}\right)^2} - \left(3\frac{\lambda_L}{L}\right)} \qquad [4]$$

where λ_L is the longitudinal dispersivity [L], and L is the length of the lysimeter [L]. Finally, the estimated mean water flow velocity v^*_0 [L T^{-1}], the estimated mean water flux q^*_0 [L T^{-1}], and the estimated mean water content θ^*_0 are given by

$$v_0^* = \frac{L}{t_0^*} \qquad [5]$$

$$q_0^* = \frac{\dfrac{t_0^*}{t_{q2}-t_{p1}}\displaystyle\sum_{t_{p1}}^{t_{q2}} V(t_i)}{t_0^*} = \frac{Q_0^*}{t_0^*} \qquad [6]$$

$$\theta_0^* = \frac{q_0^*}{v_0^*} \qquad [7]$$

where V [L] is the discharge of the lysimeter (based on the surface area of 1 m^2) during the specific observation period t_i [T], and Q^*_0 [L] is the mean measured discharge from the lysimeter (based on the surface area of 1 m^2) during the specific time period (from t_{p1} to t_{q2}) relative to the mean transit time.

Numerical Modeling

The processes in the unsaturated zone of the lysimeters were simulated using the HYDRUS-1D software package (Šimůnek et al., 2008). This numerical model considers variably saturated water flow, root growth, root water uptake, heat transport, and solute transport. The solute transport module was modified to account for isotope transport. We assumed that we can neglect fractionation processes and that the relative concentration of isotopes (δ content) does not accumulate at the upper boundary due to evaporation. This is in contrast to the standard treatment of solutes during evaporation in HYDRUS-1D, where solutes stay behind in the soil while water is removed.

Water Flow with Snow Hydrology

Variably saturated water flow was calculated using the Richards equation:

$$\frac{\partial\theta}{\partial t} = -\frac{\partial q}{\partial z} = \frac{\partial}{\partial z}\left[K(h)\frac{\partial h}{\partial z} + K(h)\right] - S \qquad [8]$$

where z is the depth below soil surface (positive upward) [L], q is the water flux [L T^{-1}], t is time [T], S is a sink term representing root water uptake [T^{-1}], and $K(h)$ is the soil hydraulic conductivity [L T^{-1}], which is a function of pressure head h [L] and volumetric water content θ. The water retention characteristic θ(h) and the hydraulic conductivity function $K(h)$ were described as suggested by van Genuchten (1980) and Mualem (1976):

$$\theta(h) = \begin{cases} \theta_r + \dfrac{\theta_s - \theta_r}{\left(1+|\alpha h|^n\right)^m} & h<0 \\ \theta_s & h \geq 0 \end{cases} \qquad [9]$$

$$K(h) = K_s \frac{[1-(\alpha h)^{n-1}[1+(\alpha h)^n]^{-m}]^2}{[1+(\alpha h)^n]^{\frac{m}{2}}} \qquad [10]$$

where θ_s and θ_r are the saturated and residual water contents, respectively; α [L^{-1}], n, and m (= 1 − 1/n) are empirical parameters defining the shape of the retention curves, and K_s is the saturated hydraulic conductivity [L T^{-1}]. Scaling factors (α_θ) were used to adjust different saturated water contents at different depths of individual soil horizons based on measured water contents (Vogel et al., 1991). The depths to which these scaling factors were assigned were chosen in the middle between measurement points.

Snow normally occurs during the winter season in the observation area. Snow cover was modeled using a simplified approach (e.g., Jarvis, 1994) that assumed that precipitation during periods with below zero temperatures was in the form of snow and did not immediately infiltrate the soil. Snow melt was then simulated, assuming that it is proportional to the air temperature above freezing, using a degree-day snow melting constant of 0.43 cm d^{-1} K^{-1} (e.g., Jarvis, 1994). This melting constant indicates what amount of snow melts during 1 d for each degree above freezing.

Root Water Uptake, Root Growth, and Plant Development

Root water uptake was simulated using the Feddes model with different stress response functions depending on the vegetation type, which are available in the HYDRUS-1D code (Šimůnek et al., 2008). Root depths were observed down to 60 to 100 cm for all three kinds of plants (Bohner et al., 2007). For the lysimeter with grass, the root depth was assumed to be constant (60 cm). For the other crops, a linear increase in root depth was assumed. Root growth started in spring, based either on the sowing date (maize) or the spring temperature increase (rye). A maximum rooting depth of 100 cm was reached in the mid season (approximately the end of July) when the plants were fully developed. After that, the root length was assumed to be constant until the harvest. Similarly, plant growth and LAI were assumed to increase linearly during the growing phase and be constant thereafter. The estimated LAI was used to separate the evaporation and transpiration rates from ET_p using an extinction coefficient of 0.6 (Ritchie, 1972).

Isotope Transport

Assuming a single porous medium (all water considered to be mobile), solute transport is described using the advection-dispersion equation:

$$\frac{\partial(\theta C)}{\partial t}=\frac{\partial}{\partial z}\left(\theta D\frac{\partial C}{\partial z}\right)-\frac{\partial(qC)}{\partial z}-SC \qquad [11]$$

where C [M L^{-3}] is the tracer concentration, D is the dispersion coefficient [L^2 T^{-1}], and S is the root water uptake [T^{-1}] from Eq. [8]. Note that the last term accounts for the passive root solute uptake. For one-dimensional transport, D is defined according to Bear (1972):

$$D=\frac{\lambda_L q}{\theta}+D_w\tau_w \qquad [12]$$

where λ_L is the longitudinal dispersivity [L], D_w is the molecular diffusion coefficient in free water [L^2 T^{-1}] (10^{-9} m^2 s^{-1}), and τ_w is the tortuosity factor.

However, when the delta notation is used (see Eq. [1]), water isotopes cannot be treated in the same way as other solutes or tracers. For example, water isotope contents do not increase in the infiltrating water due to evaporation, as other solutes do. As we can neglect any fractionation effect due to evaporation (as will be discussed later), the relative isotope content in the infiltrating water remains constant and is independent of the evaporation rate. The code for solute transport was therefore modified at the upper boundary; that is, evaporation had no effect on the solute concentration (on the isotope delta content). While water leaves the soil profile (evaporates) and solutes stay behind (and concentrate at the upper boundary) in the standard treatment of evaporation, both water and isotopes can leave at the same rate in the modified code. As with the transpiration process, the isotope content taken up by roots is equal to the solute concentration, without having a fractionation effect (Zimmermann et al., 1967; Allison et al., 1984). This option was already available in HYDRUS-1D to allow for passive root solute uptake.

Inverse Modeling and Parameter Estimation

"Atmospheric boundary condition with a surface layer" and "seepage face" were used as upper and lower boundary conditions (BCs) for water flow, respectively. Both boundary conditions involve both Neumann and Dirichlet BCs, which are used alternatively depending on conditions in the soil. For the upper boundary, the Neumann boundary condition is used as long as the surface pressure head is within a prescribed pressure head interval, and the Dirichlet boundary condition is used once the limits of this interval are reached. The "seepage face" lower boundary condition implies that the bottom water flux (a Neumann BC) is equal to zero as long as the bottom of the soil profile is unsaturated (h < 0) and that the Dirichlet BC (h = 0) is used when the bottom becomes saturated and water flux is calculated. Cauchy and Neumann boundary conditions were used for solute transport at the top and bottom of the soil profile, respectively. The Neumann BC implies that only convective solute flux occurs at the outflow boundary.

Water retention characteristics were determined in the laboratory using soil core samples taken in the field. However, water contents measured in the laboratory were higher at the same pressure heads than those measured in situ in the lysimeters, indicating that lab measurements were not representative of field conditions. Therefore, soil hydraulic parameters were determined using the inverse option (Marquardt–Levenberg optimization algorithm) of HYDRUS-1D to parameterize the model. Initial estimates of soil hydraulic parameters (Eq. [9] and [10]) were determined for each horizon from about 190 in situ measured water content–pressure head points covering a wide range of pressure heads (from a maximum of −10 cm to a minimum of −1000 cm) in 2007. The residual water content was set to zero to reduce the number of fitting parameters. To avoid compensating effects of parameters from different horizons during the optimization process, the parameter estimation was accomplished in a stepwise procedure. During the first three steps, soil hydraulic properties were successively determined for the three soil horizons, starting with the top A_p horizon, while considering in the objective function only measured variables for a particular horizon. The objective function included water contents in relevant depths during the last

2 yr of the experiment (except for the winter period when the soil was frozen), water retention characteristics measured in situ 1 yr after the observation period, and saturated hydraulic conductivities investigated in the laboratory using column experiments. During the fourth step, the parameters of all soil horizons were refined, considering additionally also the cumulative bottom discharge in the objective function. During the fifth step, dispersivities were inversely determined using the measured isotope contents in the discharge in the objective function. As $\delta^{18}O$ contents were measured only in the discharge, data were not sufficient to inversely fit dispersivities for each soil horizon. Therefore, only an apparent longitudinal dispersivity for the entire lysimeters was estimated.

Modeling Efficiency

The Nash–Sutcliffe efficiency (NSE) (Nash and Sutcliffe, 1970) was used to determine the goodness of the modeling:

$$\mathrm{NSE}=1-\frac{\sum_{t=1}^{T}\left[\xi_o(t)-\xi_m(t)\right]^2}{\sum_{t=1}^{T}\left[\xi_o(t)-\overline{\xi_o}\right]^2} \qquad [13]$$

where ξ_o and ξ_m are the observed and simulated values at a given time t, and $\overline{\xi_o}$ is the mean observed value over the entire observation period. Efficiencies close to 1 indicate a good simulation result. Efficiencies of zero or smaller indicate that the model is only as good as or even worse than the mean observed value, respectively. The goodness of the simulation was determined by comparing observed and simulated water contents, discharge, and $\delta^{18}O$.

Additionally, the coefficient of determination was computed to evaluate if there is a linear relationship ($R^2 = 1$) between calculated and measured values.

$$R=\left\{\frac{\sum_{t=1}^{T}\left[\xi_o(t)-\overline{\xi_o}\right]\left[\xi_m(t)-\overline{\xi_m}\right]}{\sqrt{\sum_{t=1}^{T}\left[\xi_o(t)-\overline{\xi_o}\right]^2\cdot\sum_{t=1}^{T}\left[\xi_m(t)-\overline{\xi_m}\right]^2}}\right\}^2 \qquad [14]$$

where $\overline{\xi_m}$ is the mean simulated value over the entire observation period.

Results and Discussion

Water Balance

Impact of Land Cover

The lowest discharge was observed in the grass–clover lysimeter and the highest in the maize lysimeter treated with cattle slurry (Table 1). On average, the discharge decreased from maize (2537 ± 247 mm) to rye (2466 ± 42 mm) to grass (2264 mm). This was likely caused by the length of the vegetation period for different crops and resulting differences in root water uptake. However, the difference in discharge between two maize lysimeters was also quite large, with lower discharge from the lysimeter treated with animal manure. The application of fertilizers or differences in the actual infiltration rates may thus cause differences in drainage, which will be discussed later. When comparing lysimeters with the same crops (Lys1 and Lys2, or Lys3 and Lys4), and thus with the same duration of the vegetation period, differences in observed discharge were more distinct for the same crops in 2004 (Fig. 1) than in other years. Here, the total discharge was higher in Lys1 and Lys4 than in Lys2 and Lys3, which was caused by higher discharge in spring during snow melt (Lys1 and Lys4) and higher discharge in late autumn (Lys1). The same effect was found for the rye lysimeters in 2005 (Fig. 1b). Differences in the spring during snow melt can be caused either by different contributions of preferential flow and infiltration due to partially frozen soils (Stähli et al., 1996) or by different infiltration into lysimeters due to runon–runoff processes during snow melt (Bayard et al., 2005).

Impact of Fertilization Method

Less total discharge was observed in the soils treated with animal manure (Fig. 1a,b). However, this only holds true if the total observation period is considered. When comparing only the data till 2006, there is no apparent trend between different fertilization methods, as higher discharge was measured both from maize lysimeters with cattle slurry and from rye lysimeters with animal manure. Animal manure generally has a higher organic matter content than cattle slurry (Antil et al., 2005) and can thus bind more water near the soil surface, making it readily available for evapotranspiration. Also, organic matter has lower density than the soil material itself, proportionally decreasing the bulk density and increasing aggregate stability (MacRae and Mehuys, 1985), thereby

Table 1. Water balance, mean isotope contents in precipitation and discharge, and estimated flow parameters: precipitation P, discharge Q, mean water flux q, and evapotranspiration ET. All values are for the duration of the experiments (i.e., a 5-yr period).

	Crop	Fertilizer	P or Q	q	$\mathrm{ET_{ref}}$†	$\mathrm{ET_a}$‡	$\delta^{18}O$	$\delta^{2}H$
			mm	mm d^{-1}	——mm——		——‰——	
Precipitation			5182	2.99	3170		−9.86	−72.8
Discharge								
Lys1	maize	liquid cattle slurry	2711	1.56		2376	−10.29	−78.8
Lys2	maize	solid animal manure	2362	1.36		2788	−10.27	−79.4
Lys3	winter rye	liquid cattle slurry	2496	1.44		2576	−10.09	−77.1
Lys4	winter rye	solid animal manure	2436	1.40		2654	−10.37	−79.3
Lys5	grass–clover	mineral PK	2264	1.30		2816	−9.64	−73.1

† Potential reference evapotranspiration according to FAO-56 (Allen, 2000).
‡ Actual evapotranspiration calculated with HYDRUS.

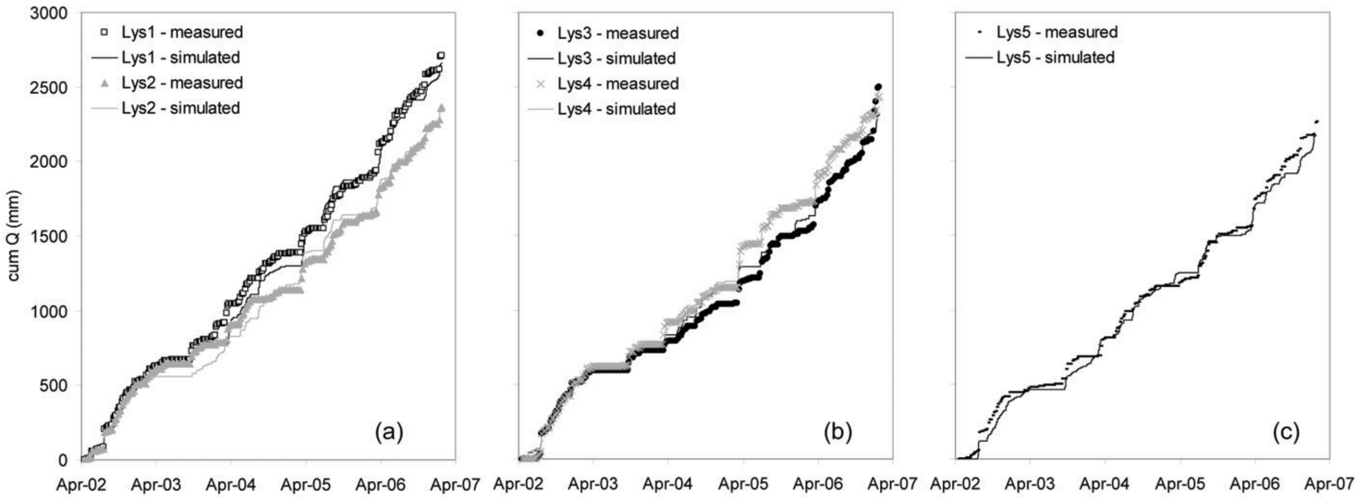

Fig. 1. Measured (symbols) and simulated (line) cumulative discharge for (a) the maize lysimeters, (b) the rye lysimeters, either treated with cattle slurry (black) or animal manure (gray), and (c) the grass–clover lysimeter.

producing differences in soil hydraulic properties. Increased organic matter contents not only affect water flow, but also impact sorption processes (e.g., Celis et al., 2006), which additionally need to be considered when investigating reactive transport.

To summarize the water balance analysis, differences in discharge rates may be caused by (i) local structural heterogeneities or differences in soil hydraulic properties, resulting in preferential flow during snow melt; (ii) different infiltration amounts due to runon–runoff processes; (iii) different duration of plant growth periods; or (iv) different fertilization methods.

Soil Hydraulic Properties

Impact of Land Cover

Although the lysimeters contained undisturbed material, all water contents measured in situ in the lysimeters were lower ($\Delta\theta = 0.14$–0.26) than water contents measured at similar pressure heads in drainage experiments in the lab (Table 2). This indicates a possible soil compaction during the installation of the lysimeters. Field measured water contents can also be lower than lab measurements due to entrapped air. It was found previously that field-measured water contents were about 20 to 30% lower than lab measurements due to entrapped air (Coquet et al., 2005). From the measured water contents and pressure heads, three different soil horizons were identified, which varied in depths within the five lysimeters (see modeling results). Water retention functions for soils in the A_p horizon of the two rye lysimeters were almost parallel (Fig. 2b) and similar to those in the grass lysimeter (Fig. 2c). However, soils in the maize lysimeters had retention curves of two different shapes (Fig. 2a). In the deeper B_v soil horizon, the in situ measured water retention curves were almost parallel for all five lysimeters, with little variability in observed water contents (Fig. 3). In the C_v horizon, only a narrow range of pressure heads (from −30 to −80 cm) and small differences in water contents (±0.01–0.03) were observed (Fig. 4). This was mainly due to the imposed bottom boundary condition (i.e., seepage face), which keeps moisture conditions close to full saturation. Besides, the effects of root water uptake in upper horizons significantly smoothed variations in flux related variables at greater depths. Generally, the smallest water contents were measured in the maize lysimeters (Fig. 2a–4a) and the largest in the rye lysimeter treated with animal manure (Fig. 2b–4b).

Impact of Fertilization Method

The higher amount of the organic matter in soils treated with animal manure also resulted in a relative increase of porosity (and water contents) in the upper soil layer in Lys2 and Lys4 (Fig. 2).

Table 2. Soil properties measured in laboratory experiments on samples collected near the location were the undisturbed lysimeters were taken, including bulk density ρ_b, porosity n, gravels, sand, silt, clay, saturated hydraulic conductivity K_s, water content θ, and pressure head h.

Soil horizon	ρ_b	n	Gravels	Sand	Silt	Clay	K_s	$\theta(h)$							
cm	g cm^{-3}		%	%	%	%	cm d^{-1}	−10 cm	−30 cm	−60 cm	−100 cm	−300 cm	−800 cm	−3000 cm	−15000 cm
0–25	1.17	0.56	16.4	36.8	36.8	10	946	0.46	0.42	0.39	0.36	0.33	0.29	0.21	0.11
25–80	1.32	0.51	16.2	37.7	35.2	10.9	188	0.41	0.38	0.35	0.33	0.30	0.27	0.19	0.10
80–110	1.25	0.54	20.7	38.9	32.5	7.9	175	0.44	0.41	0.38	0.36	0.32	0.29	0.20	0.12
110–150	1.53	0.44	34.0	48.2	15.8	2	673	0.30	0.25	0.22	0.20	0.15	0.13	0.10	0.06

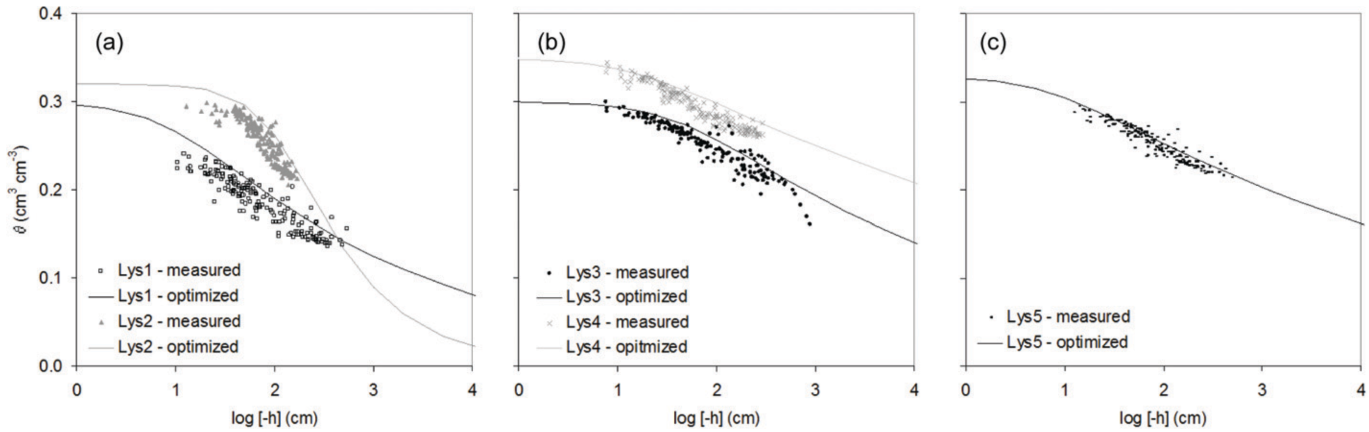

Fig. 2. Measured (symbols) and optimized (lines) water retention functions in the A_p horizon of (a) the maize lysimeters, (b) the rye lysimeters, either treated with cattle slurry (black) or animal manure (gray), and (c) the grass–clover lysimeter.

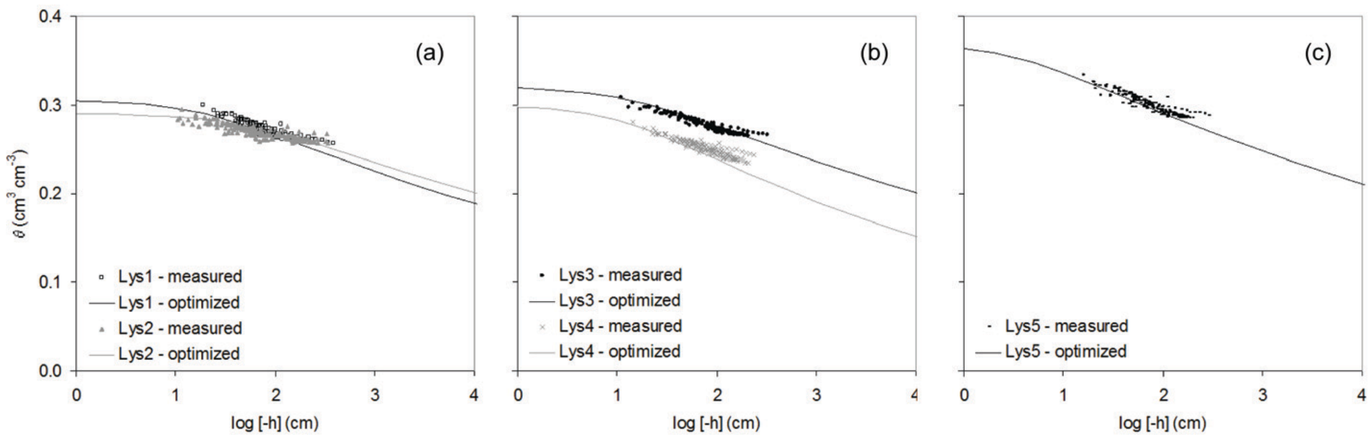

Fig. 3. Measured (symbols) and optimized (lines) water retention functions in the Bv horizon of (a) the maize lysimeters, (b) the rye lysimeters, either treated with cattle slurry (black) or animal manure (gray), and (c) the grass–clover lysimeter.

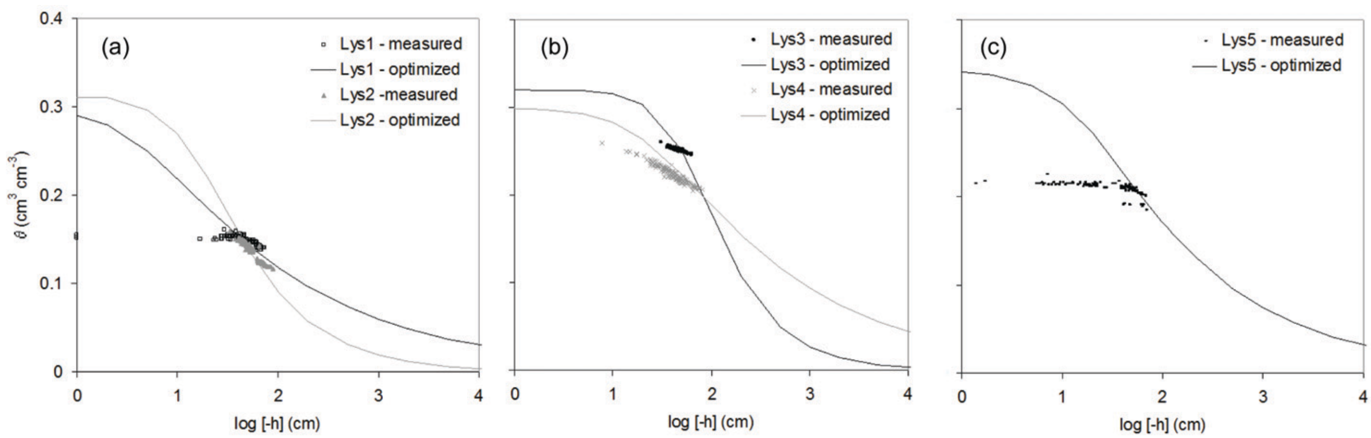

Fig. 4. Measured (symbols) and optimized (lines) water retention functions in the C_v horizon of (a) the maize lysimeters, (b) the rye lysimeters, either treated with cattle slurry (black) or animal manure (gray), and (c) the grass–clover lysimeter.

As mentioned above, it is known that bulk densities decrease and porosities increase correspondingly, depending on the rates of manure amendment (Miller et al., 2002; Fares et al., 2008). The maize lysimeter with animal manure not only displayed larger water contents and storage capacities, but as already mentioned above, also a different shape of the retention function. As this was not observed for the rye lysimeter, this may have been an effect of local structural heterogeneities rather than an impact of different treatments.

These in situ measured water contents indicate that differences in physical parameters due to fertilizer application and land cover, such as water contents and porosities, are restricted to the upper 30 cm of the soil profile, which is in agreement with other studies (Schwartz et al., 2003; Ndiaye et al., 2007). At greater depths, temporal variations of water contents are caused mainly by structural heterogeneities rather than soil treatment or plant growth.

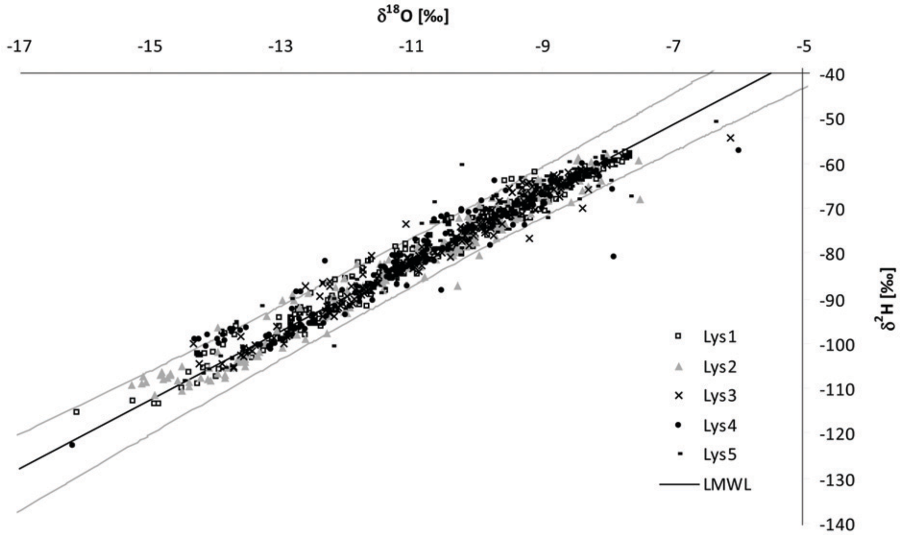

Fig. 5. Isotopic compositions in precipitation (expressed as the local meteoric water line, LMWL) and in the lysimeter discharge.

Stable Isotopes of Water

Both $\delta^{18}O$ and $\delta^{2}H$ were measured in water samples of the lysimeter discharge. Note that the isotopic compositions of the discharge, plotted with the local meteoric water line (LMWL, Fig. 5), indicated a negligible fractionation effect due to evaporation. Therefore, we only considered $\delta^{18}O$ as a tracer in the analysis since more data were available for this isotope. Nevertheless, using $\delta^{2}H$ would have resulted in the same results and conclusions. Water isotope contents in precipitation showed seasonal variation, with daily inputs between 0 and −30‰ for $\delta^{18}O$ (Fig. 6), with mean weighted contents for the entire observation period of 5 yr of −9.86 and −72.8‰ for $\delta^{18}O$ and $\delta^{2}H$, respectively (Table 1). Mean weighted summer and winter isotope contents in precipitation were −8.31 and −60.5‰ for $\delta^{18}O$ and $\delta^{2}H$ and −12.85 and −96.4‰ for $\delta^{18}O$ and $\delta^{2}H$, respectively.

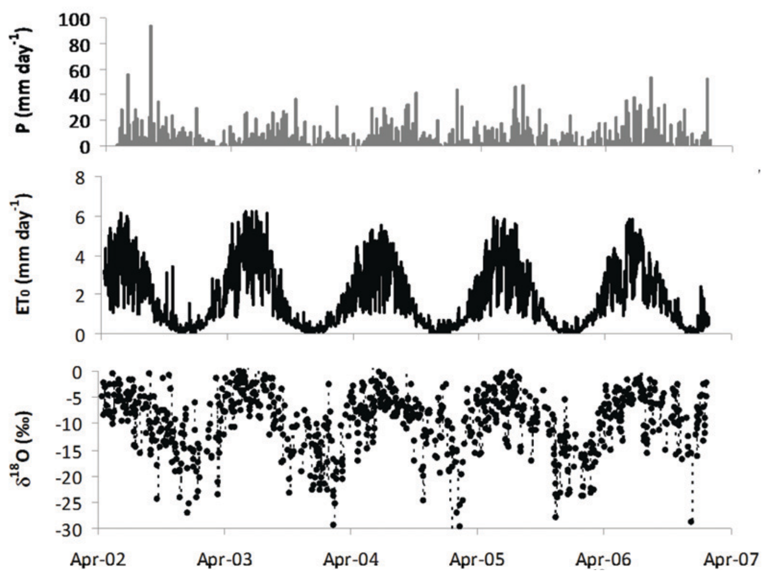

Fig. 6. Precipitation, calculated grass reference evapotranspiration, and $\delta^{18}O$ contents in precipitation.

Impact of Land Cover

The mean weighted isotope contents from the discharge are given in Table 1. The mean isotope contents of the crop lysimeters (Lys1–4) were generally smaller than in the precipitation. This indicates a higher contribution of winter precipitations, which have smaller isotope contents than summer precipitations, to the discharge in the crop lysimeters compared to the grass lysimeter. Lys1–4 remained bare in autumn and winter, and therefore less water was lost by evapo(transpi)ration. For the grass–clover lysimeter (Lys5), the weighted mean isotope contents were close to the precipitation contents, indicating a closer resemblance of the annual course of precipitation and ET than for the other lysimeters. Thus, the mean isotope content in the discharge reflects the seasonal origin of recharging water, depending on the vegetation.

The seasonal distribution, albeit with smaller amplitudes than in precipitation due to weekly sampling and dispersion (from −8 to −16‰ for $\delta^{18}O$), was also observed in the water isotopes of the lysimeters discharge (Fig. 7); it was similar in all lysimeters. However, water fluxes seemed to be highly variable throughout the whole observation period, as a clear periodic signal in precipitation was echoed in the irregular and erratic signal in the discharge. In the lysimeters planted with rye (Lys3, Lys4), the seasonal isotope signal was less pronounced than in the lysimeters planted with maize, indicating higher dispersivities. The isotope distribution in the discharge was also less smooth than in other lysimeter studies (Maloszewski et al., 2006; Stumpp et al., 2009a,c). In one of these studies (Stumpp et al., 2009a), isotope contents in the discharge of two lysimeters, containing the same soil and either planted

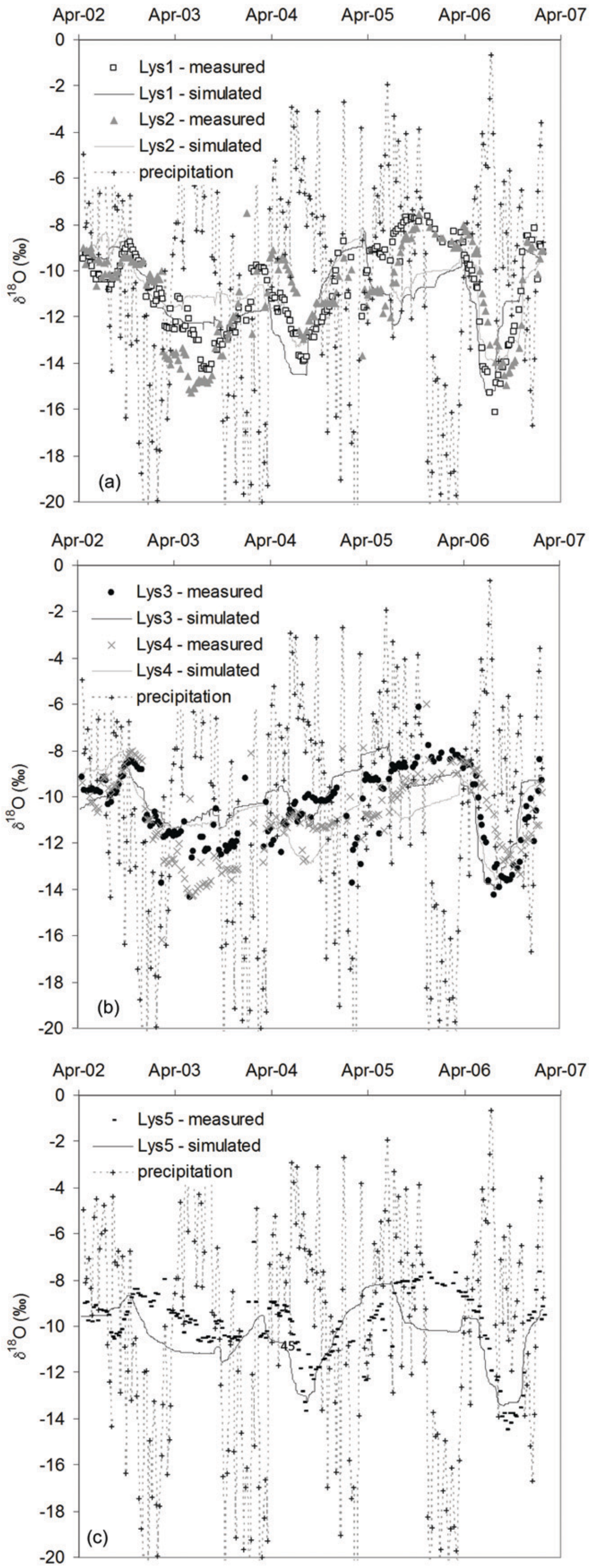

Fig. 7. Measured (symbols) and calculated (lines) $\delta^{18}O$ contents in the discharge of (a) the maize lysimeters, (b) the rye lysimeters, either treated with cattle slurry (black) or animal manure (gray), and (c) the grass/clover lysimeter.

with maize or crop rotation, was much smoother. However, these lysimeters also revealed differences in seasonal peaks of isotope contents and in water fluxes with respect to the vegetation (Stumpp et al., 2009a). In this previous study, the seasonality was more pronounced in the maize lysimeter, which had greater fluxes and thus correspondingly higher pore water velocities. Although such obvious differences between vegetation covers were not found in the present study, more complex differences in water flow velocities (transit times) and transport parameters were observed. These may have been caused by a combination of several factors, including structural heterogeneities, water flow variability, and/or different plant growth.

Impact of Fertilization Method

A clear trend in the mean values and the temporal distribution of isotope contents is absent when comparing different fertilizer applications.

Estimation of Mean Flow Parameters

Impact of Land Cover

Mean transit times determined from the peak shift of the depleted winter precipitation of 2005–2006 were shorter in the maize lysimeters than in the rye lysimeters (Table 3), although the discharge during this time period was greater in the rye lysimeters (Table 3). Consequently, mean water flow velocities were faster in the maize lysimeters than in the rye lysimeters. In the grass lysimeter, mean transit times were between those calculated for the maize and rye lysimeters (Table 3). By analyzing the water balance alone, one would conclude that transit times in the rye lysimeter are faster than in the maize lysimeters. Only the environmental tracers provide evidence of actual transit times. This is due to small differences in the effective mean water contents, emphasizing the importance of this variable. The estimated mean water contents were similar, ranging from 0.265 to 0.280, with smaller values calculated for the maize lysimeters compared to the rye lysimeters (Table 3). These small differences in water contents still produced significant differences in mean transit times. The estimated water contents corresponded well with measured water contents at all depths (Fig. 2, 3, 4).

Impact of Fertilization Method

Calculated mean transit times were shorter for the lysimeters with the application of cattle slurry (Lys1, 3) than in the lysimeters with the animal manure application (Lys2, 4), which is in agreement with the higher discharge rates in Lys1 and Lys3 compared to lower rates in Lys2 and Lys4. This again supports the notion that higher organic contents from solid animal manure remain in the upper soil and increase the water storage capacity easily available for evapotranspiration, resulting in smaller mean water flow velocities.

In general, mean flow parameters estimated from the stable isotopes of water clearly elucidate differences between the lysimeters, providing evidence of the impact of land cover and

Table 3. Estimated mean flow parameters: mean concentration peak shift time t_m^*, mean transit time t_0^*, mean water volume Q_0^*, mean water flow velocity v_0^*, mean water flux q_0^*, and mean water content θ_0^* determined from the peak shift of the depleted winter precipitation peak of 2005–2006.

Lysimeter	t_m^*	t_0^*	Q_0^*	v_0^*	q_0^*	θ_0^*
	d		mm	mm d^{-1}		
Lys1	196	212	405	7.1	1.9	0.271
Lys2	214	229	398	6.6	1.7	0.265
Lys3	228	250	410	6.0	1.6	0.274
Lys4	249	272	417	5.5	1.56	0.278
Lys5	224	244	420	6.1	1.7	0.280

fertilization method. This is not obvious from water balance and mean discharge rates alone.

Modeling Water Flow and Isotope Transport

Inversely determined soil hydraulic and solute transport parameters are summarized in Table 4. The optimized water retention characteristics are presented in Fig. 2 through 4. The optimized retention function for the C_v horizon of Lys5 indicated much higher water contents close to saturation than actually measured (Fig. 4c). However, using a saturated water content of about 0.20 cm^3 cm^{-3} was too small, and thus, model accuracy decreased compared to the simulations using the fitted retention function with a saturated water content of 0.34 cm^3 cm^{-3}.

Estimated saturated hydraulic conductivities (Table 4) varied three orders of magnitude (about 10^1–10^3 cm d^{-1}) in the A_p horizon. The range of K_s was independent of land use and did not increase with increasing water contents due to the manure application as shown in Fares et al. (2008). However, the lysimeters with the smallest K_s in the A_p horizon (Lys2 and Lys3) also had the lowest α (Table 4), likely indicating a strong correlation between these two parameters. K_s values for the B_v and C_v horizons also did not show any trend with respect to fertilizer application or land cover and exhibited less variation than for the A_p horizon. Note that full saturation was never reached in these soils, and thus the saturated hydraulic conductivity is far beyond the range of inversely determined values. Consequently, differences between the lysimeters in the soil hydraulic conductivity function in the interval of actually measured water contents were much less pronounced.

While simulated discharge and water isotope contents corresponded well with measured values, the goodness of fit for water contents was not particularly good and varied with depths, with generally higher NSE in the upper 25 cm (Table 5). While we report in Table 5 NSE for all lysimeters and all depths, we believe that the NSE is not a particularly useful measure when measured water contents vary in a very narrow range (often within the precision of measurements), with measured values most of the time close to their mean values. The denominator in Eq. [13] is then very small, resulting in low NSE, particularly in deeper soil layers where water contents stayed more or less constant over time. Although

Table 4. Optimized soil hydraulic and transport parameters for the five lysimeters; note θ_r was set zero to reduce the number of optimized parameters.

		z	θ_r	θ_s	α	n	K_s	λ_L
		cm			cm^{-1}	–	cm d^{-1}	cm
Lys1	A_p	0–25	0	0.30	0.112	1.186	639	3.9
	B_v	26–97	0	0.31	0.057	1.076	434	3.9
	C_v	98–150	0	0.30	0.235	1.294	1034	3.9
Lys2	A_p	0–30	0	0.32	0.008	1.607	6.2	3.4
	B_v	31–97	0	0.29	0.019	1.070	1179	3.4
	C_v	98–150	0	0.31	0.060	1.678	236	3.4
Lys3	A_p	0–30	0	0.30	0.023	1.140	110	4.7
	B_v	31–90	0	0.32	0.076	1.070	6000	4.7
	C_v	91–150	0	0.32	0.016	1.900	110	4.7
Lys4	A_p	0–30	0	0.35	0.067	1.080	1790	4.6
	B_v	31–85	0	0.30	0.092	1.100	4150	4.6
	C_v	86–150	0	0.30	0.038	1.320	276	4.6
Lys5	A_p	0–25	0	0.33	0.146	1.098	935	4.3
	B_v	86–97	0	0.37	0.307	1.070	550	4.3
	C_v	98–150	0	0.34	0.063	1.369	694	4.3

Table 5. Nash–Sutcliff efficiencies (NSE) and coefficient of determination (R^2) determined by comparing measured and simulated weekly discharge rates, isotope contents in the discharge, and water contents.

			Water content						
	Q	$\delta^{18}O$	10 cm	15 cm	25 cm	45 cm	70 cm	100 cm	130 cm
	NSE								
Lys1	0.25	0.37	0.17	0.29	0.26	0.16	−0.11	−1.58	−0.17
Lys2	0.52	0.21	0.28	0.10	0.13	0.18	0.23	0.02	0.12
Lys3	0.60	0.34	0.22	0.26	0.46	0.18	0.23	−0.40	0.06
Lys4	0.69	0.14	−0.04	0.38	0.36	−0.25	nd†	0.40	−1.93
Lys5	0.67	0.31	−0.26	−0.27	0.02	−0.71	−9.51	0.05	−2.69
	R^2								
Lys1	0.41	0.44	0.25	0.37	0.49	0.42	0.29	0.13	0.04
Lys2	0.57	0.28	0.27	0.32	0.29	0.59	0.65	0.57	0.57
Lys3	0.62	0.41	0.20	0.25	0.51	0.61	0.62	0.18	0.73
Lys4	0.74	0.24	0.21	0.39	0.46	0.57	nd	0.61	0.53
Lys5	0.68	0.47	0.34	0.39	0.52	0.50	0.33	0.55	0.57

† nd, water content was not determined.

water contents were generally well represented by the model, this cannot be concluded in this case from the NSE. For example, differences between measured and simulated water contents in the depth of 130 cm in Lys5 were small, varying between 0 and 0.015 $cm^3 cm^{-3}$ throughout the entire observation period. Here, the average measured water content (0.279 $cm^3 cm^{-3}$) was only about 0.01 $cm^3 cm^{-3}$ higher than the simulated average value (0.267 $cm^3 cm^{-3}$). Such low differences in water contents between measured and simulated values are in the range of precision for TDR measurements (0.01 $cm^3 cm^{-3}$) (Evett et al., 2006). Thus, the NSE does not provide a full picture about the modeling results when simulating variables that vary within a narrow range of values. Note that the NSE measure (Nash and Sutcliffe, 1970) was specifically designed for evaluating dynamic rather than static variables (i.e., fluxes/discharge rather than water contents). Therefore, we additionally calculated coefficients of determination (R^2) indicating that simulated water contents generally are in good agreement with measured ones (Table 5), particularly in the depths below 25 cm.

The results of the isotope transport modeling are presented in Fig. 7. The best modeling efficiencies were obtained for the simulations in the lysimeters with cattle slurry and in the grass lysimeter (Table 5). Particularly, at the end of the observation period (after April 2006), simulated and measured isotopes in the discharge were in good agreement. We found that the apparent dispersivity was smallest for the maize lysimeters and greatest for the rye lysimeter (Table 4). In a similar study (Stumpp et al., 2009a), higher dispersivities were found in the 150 cm deep lysimeter with crop rotation (8.1 cm) than with maize monoculture (6.8 cm); however, they were about two times higher than in the present study (3.4–4.7 cm), which might be caused by the finer texture of the soil in the previous study (10% more clay). Nevertheless, the dispersivities were all in the same range, emphasizing the intrinsic nature of this soil. The optimized values, although low, are comparable to values found for similar experimental setups (Vanderborght and Vereecken, 2007), indicating more homogeneous transport behavior (less spreading). Vanderborght and Vereecken (2007) reported dispersivities ranging from 2 to 20 cm for field and column experiments with 80- to 200-cm transport distance and water fluxes smaller than 10 mm d^{-1}. On average, dispersivities of about 5 cm were found in experiments with similar transport distance (80–200 cm) in coarse sediments compared to about 9 cm in finer sediments (Vanderborght and Vereecken, 2007).

Main discrepancies between simulated and measured values can be generally attributed to uncertainties related to infiltration during snow melt. The actual quantity and timing of infiltrating water often remain unknown in soils where soil frost, snow cover, and snow melt may play a crucial role. Snow drift and irregular thawing of soil may produce differences in the infiltration pattern. Furthermore, surface runon and runoff processes in agricultural fields may cause patchy and nonuniform infiltration patterns as the soil close to the surface can be partly frozen during snow melt events, none of which is considered by the model or can be actually measured. For example, the isotope content of infiltrating water from the melting snow layer remains unknown and differs from the contents of fresh snow. It was shown that diffusion processes in the vapor phase resulted in the homogenization of isotope contents in the snow layer (Herrmann et al., 1981; Stichler and Schotterer, 2000). Besides, the first melt water is always more depleted in isotopes than the initial content due to fractionation (Herrmann et al., 1981). In the same study it was shown that isotopic exchange between the rainwater and the snow layer is on the order of 10%. Thus, the isotope content is different for rainwater when it infiltrates into the soil through a snow layer. Snow lysimeters would be required to determine the isotope content of the actual infiltrating water to account for isotope effects in snow layers and improve the modeling results.

To conclude, simulations indicate that numerical modeling can reproduce the general trend of water flow and isotope transport, but more data, such as pressure heads in the same depths as water content measurements and isotope contents of snow melt infiltration, would be required to improve its accuracy. Furthermore, soil frost and surface runon–runoff processes during snow melt may have been crucial processes that were not considered by our model. Our results indicate that patchy infiltration patterns may vary over time and play a crucial role in water flow and transport processes on the plot scale. Also, structural heterogeneities can result in water flow heterogeneities impacted by land cover and fertilizer application. Both heterogeneous infiltration patterns and flow heterogeneities not only occur in our study, but are general phenomena that need to be implemented in transport models to better predict atmosphere–plant–soil–groundwater interactions under variable flow conditions. Even under steady-state irrigation conditions, highly heterogeneous flow patterns were observed for tracer experiments in a sandy loam that was formerly used for agricultural purposes (Öhrstrom et al., 2004). Similar results were observed by Williams et al. (2003), who found spatial flow variability, including preferential flow patterns, in a grass field during steady-state irrigation experiments.

Summary and Conclusions

Soil hydraulic parameters, lysimeter discharge rates, water isotopes, and mean transit times were used to determine the influence of land cover and fertilizer application on water flow and solute transport. Five lysimeters containing undisturbed soil monoliths were taken from and placed at the same agricultural field site. Maize, winter rye, and grass–clover were planted over a period of 5 yr. Lysimeters with maize and rye were each treated with liquid cattle slurry or solid animal manure, while a PK fertilizer was used for the grass lysimeter.

The largest discharge was measured in the maize lysimeter with the cattle slurry application, and the smallest in the grass lysimeter. The main differences in discharge between the five lysimeters were observed in spring and during the plant growth periods, indicating the importance of runon–runoff processes during snow melt and root water uptake, respectively. The crucial role of patchy infiltration patterns during snow melt was also obvious from water isotope contents in the discharge and from inaccurate model simulations during this time period.

In situ water content measurements indicated an impact of the different fertilization treatments on the soil structure in the upper 25 to 30 cm. In particular, water retention functions were different for the maize lysimeters, indicating higher porosities and water storage capacities for soils treated with manure amendments in comparison to those treated with cattle slurry. Furthermore, fitted K_s of the upper soil horizons varied by about three orders of magnitude between the lysimeters. However, an obvious impact due to plants or treatments causing these great differences in K_s cannot be clearly demonstrated. Below a depth of 30 cm, the shape of the water retention functions was similar in all lysimeters and only differences in porosities were found.

The seasonal signal of infiltration was attenuated, but much less smooth compared to other studies. Still, it was possible to determine mean flow parameters (water velocity, transit times, and water contents), which clearly helped to identify and quantify the impact of land cover and fertilization method, emphasizing the added value of using water isotopes as an environmental tracer in long-term studies. Smaller mean transit times were found in the maize lysimeters and for soils with the liquid cattle slurry application. The estimated mean water contents were in agreement with measured values. Although numerical calculations yielded good simulations, abrupt erratic changes in isotope contents in the discharge could not be adequately simulated. Nevertheless, the general trend in water flow and isotope transport was well simulated with HYDRUS-1D, which was modified to adjust the upper solute boundary conditions for isotope transport. Additionally, the simulations yielded similar dispersivities in all lysimeters, suggesting similar soil structure and less pronounced impact of land cover and fertilization method on transport compared to water flow.

Differences between the lysimeters suggest that impacts due to fertilizer application and land cover were restricted to only the upper soil horizon. However, even more important than these factors were the differences in infiltration patterns and the effect of snow melt, which were independent of fertilization method and land cover, and which had a significant influence on water flow and transport processes.

Acknowledgments

This work was supported by a fellowship within the Postdoc-Programme of the German Academic Exchange Service (DAAD). Partial support of this work through EU Genesis Project no. 226536 (FP7-ENV-2008-1) is kindly acknowledged.

References

Allen, R.G. 2000. Using the FAO-56 dual crop coefficient method over an irrigated region as part of an evapotranspiration intercomparison study. J. Hydrol. 229:27–41. doi:10.1016/S0022-1694(99)00194-8

Allen, R.G., L.S. Pereira, D. Raes, and M. Smith. 1998. Crop evapotranspiration—Guidelines for computing crop water requirements. FAO Irrigation and Drainage Paper 56. FAO, Rome.

Allison, G.B., C.J. Barnes, M.W. Hughes, and F.W. Leaney. 1984. Effect of climate and vegetation on oxygen-18 and deuterium profiles in soils. *In* Proc. Isotope Hydrology. Proc. Symp., Vienna. IAEA, Vienna, Austria.

Antil, R.S., M.H. Gerzabek, G. Haberhauer, and G. Eder. 2005. Long-term effects of cropped vs. fallow and fertilizer amendments on soil organic matter I. Organic carbon. J. Plant Nutr. Soil Sci. 168:108–116. doi:10.1002/jpln.200421461

Bachmair, S., M. Weiler, and G. Nützmann. 2009. Controls of land use and soil structure on water movement: Lessons for pollutant transfer through the unsaturated zone. J. Hydrol. 369:241–252. doi:10.1016/j.jhydrol.2009.02.031

Bayard, D., M. Stahli, A. Parriaux, and H. Fluhler. 2005. The influence of seasonally frozen soil on the snowmelt runoff at two Alpine sites in southern Switzerland. J. Hydrol. 309:66–84. doi:10.1016/j.jhydrol.2004.11.012

Bear, J. 1972. Dynamics of fluid in porous media. Elsevier, New York.

Bergkamp, G. 1998. A hierarchical view of the interactions of runoff and infiltration with vegetation and microtopography in semiarid shrublands. Catena 33:201–220. doi:10.1016/S0341-8162(98)00092-7

Bohner, A., G. Eder, and M. Schink. 2007. Nährstoffkreislauf und Stoffflüsse in einem Grünland-Ökosystem. *In* Proc. 12. Gumpensteiner Lysimetertagung. 17–18 April. Höhere Bundeslehr und Forschungsanstalt für Landwirtschaft, A-8952 Irdning.

Bormann, H., and K. Klaassen. 2008. Seasonal and land use dependent variability of soil hydraulic and soil hydrological properties of two Northern German soils. Geoderma 145:295–302. doi:10.1016/j.geoderma.2008.03.017

Celis, R., H. De Jonge, L.W. De Jonge, M. Real, M.C. Hermosín, and J. Cornejo. 2006. The role of mineral and organic components in phenanthrene and dibenzofuran sorption by soil. Eur. J. Soil Sci. 57:308–319. doi:10.1111/j.1365-2389.2005.00740.x

Chakraborty, D., R.N. Garg, R.K. Tomar, B.S. Dwivedi, P. Aggarwal, R. Singh, U.K. Behera, A. Thangasamy, and D. Singh. 2010. Soil physical quality as influenced by long-term application of fertilizers and manure under maize–wheat system. Soil Sci. 175:128–136. doi:10.1097/SS.0b013e3181d53bd7

Coquet, Y., J. Šimůnek, C. Coutadeur, M.Th. van Genuchten, V. Pot, and J. Roger-Estrade. 2005. Water and solute transport in a cultivated silt loam soil: 2. Numerical analysis. Vadose Zone J. 4:587–601. doi:10.2136/vzj2004.0153

Coutadeur, C., Y. Coquet, and J. Roger-Estrade. 2002. Variation of hydraulic conductivity in a tilled soil. Eur. J. Soil Sci. 53:619–628. doi:10.1046/j.1365-2389.2002.00473.x

Eder, G., and E. Stenitzer. 2003. Ein Vergleich von herkömmlichen Kammerlysimetern mit monolithischen Feldlysimetern. *In* Proc. 10. Gumpensteiner Lysimetertagung. 29–30 Apr. 2003. Bundesanstalt für alpenländische Landwirtschaft Gumpenstein, A-8952 Irdning.

Evett, S.R., J.A. Tolk, and T.A. Howell. 2006. Soil profile water content determination. Vadose Zone J. 5:894–907. doi:10.2136/vzj2005.0149

Fares, A., F. Abbas, A. Ahmad, J.L. Deenik, and M. Safeeq. 2008. Response of selected soil physical and hydrologic properties to manure amendment rates, levels, and types. Soil Sci. 173:522–533. doi:10.1097/SS.0b013e318182b063

Gärdenäs, A.I., J. Šimůnek, N. Jarvis, and M.Th. van Genuchten. 2006. Two-dimensional modelling of preferential water flow and pesticide transport from a tile-drained field. J. Hydrol. 329:647–660. doi:10.1016/j.jhydrol.2006.03.021

Green, S.R., M.B. Kirkham, and B.E. Clothier. 2006. Root uptake and transpiration: From measurements and models to sustainable irrigation. Agric. Water Manage. 86:165–176. doi:10.1016/j.agwat.2006.06.008

Green, T.R., L.R. Ahuja, and J.G. Benjamin. 2003. Advances and challenges in predicting agricultural management effects on soil hydraulic properties. Geoderma 116:3–27. doi:10.1016/S0016-7061(03)00091-0

Herbst, M., W. Fialkiewicz, T. Chen, T. Putz, D. Thiery, C. Mouvet, G. Vachaud, and H. Vereecken. 2005. Intercomparison of flow and transport models applied to vertical drainage in cropped lysimeters. Vadose Zone J. 4:240–254. doi:10.2136/vzj2004.0070

Herrmann, A., M. Lehrer, and W. Stichler. 1981. Isotope input into runoff systems from melting snow covers. Nord. Hydrol. 12:308–318.

Hu, W., M.G. Shao, Q.J. Wang, J. Fan, and R. Horton. 2009. Temporal changes of soil hydraulic properties under different land uses. Geoderma 149:355–366. doi:10.1016/j.geoderma.2008.12.016

IAEA. 1983. Guidebook on nuclear techniques in Hydrology. Tech. Rep. Ser. 91. IAEA, Vienna.

Jarvis, N.J. 1994. The MACRO model (Version 3.1), Technical description and sample simulations. Rep. and Diss. 19. Dep. Soil Sci., Swedish Univ. Agric. Sci., Uppsala, Sweden.

Knappe, S., U. Haferkorn, and R. Meissner. 2002. Influence of different agricultural management systems on nitrogen leaching: Results of lysimeter studies. J. Plant Nutr. Soil Sci. 165:73–77. doi:10.1002/1522-2624(200202)165:1<73::AID-JPLN73>3.0.CO;2-O

Knisel, W.G., and F.M. Davis. 2000. GLEAMS: Groundwater Loading Effects of Agricultural Management Systems, Version 3.0, user manual. USDA–ARS, Tifton, GA.

Kosmas, C., N. Moustakas, N. Kallianou, and N. Yassoglou. 1991. Cracking patterns, bypass flow and nitrate leaching in Greek irrigated soils. Geoderma 49:139–152. doi:10.1016/0016-7061(91)90097-D

Leibundgut, C., P. Maloszewski, and C. Külls. 2009. Tracers in hydrology. Wiley and Sons, West Sussex, UK.

Maciejewski, S., P. Maloszewski, C. Stumpp, and D. Klotz. 2006. Modelling of water flow through typical Bavarian soils (Germany) based on lysimeter experiments: 1. Estimation of hydraulic characteristics of the unsaturated zone. Hydrol. Sci. J. 51:285–297. doi:10.1623/hysj.51.2.285

MacRae, R.J., and G.R. Mehuys. 1985. The effect of green manuring on the physical properties of temperate-area soils. p. 71–94. *In* B.A. Stewart (ed.) Advances in soil science. Springer, New York.

Maloszewski, P., S. Maciejewski, C. Stumpp, W. Stichler, P. Trimborn, and D. Klotz. 2006. Modelling of water flow through typical Bavarian soils based on lysimeter experiments: 2. Environmental deuterium transport. Hydrol. Sci. J. 51:298–313. doi:10.1623/hysj.51.2.298

Miller, J.J., N.J. Sweetland, and C. Chang. 2002. Hydrological properties of a clay loam soil after long-term cattle manure application. J. Environ. Qual. 31:989–996. doi:10.2134/jeq2002.0989

Monteith, J.L. 1965. Evaporation and environment. Symp. Soc. Exp. Biol. 19:205–234.

Mualem, Y. 1976. A new model for predicting the hydraulic conductivity of unsaturated porous media. Water Resour. Res. 12:513–522. doi:10.1029/WR012i003p00513

Nash, J.E., and J.V. Sutcliffe. 1970. River flow forecasting through conceptual models part I—A discussion of principles. J. Hydrol. 10:282–290. doi:10.1016/0022-1694(70)90255-6

Ndiaye, B., J. Molenat, V. Hallaire, C. Gascuel, and Y. Hamon. 2007. Effects of agricultural practices on hydraulic properties and water movement in soils in Brittany (France). Soil Tillage Res. 93:251–263. doi:10.1016/j.still.2006.04.005

Öhrstrom, P., Y. Hamed, M. Persson, and R. Berndtsson. 2004. Characterizing unsaturated solute transport by simultaneous use of dye and bromide. J. Hydrol. 289:23–35. doi:10.1016/j.jhydrol.2003.10.014

Oswald, S.E., M. Menon, A. Carminati, P. Vontobel, E. Lehmann, and R. Schulin. 2008. Quantitative imaging of infiltration, root growth, and root water uptake via neutron radiography. Vadose Zone J. 7:1035–1047. doi:10.2136/vzj2007.0156

Penman, H.L. 1948. Natural evaporation from open water, bare soil and grass. Proc. Royal Soc. A 193:120–146.

Pot, V., J. Šimůnek, P. Benoit, Y. Coquet, A. Yra, and M.-J. Martinez-Cordon. 2005. Impact of rainfall intensity on the transport of two herbicides in undisturbed grassed filter strip soil cores. J. Contam. Hydrol. 81:63–88. doi:10.1016/j.jconhyd.2005.06.013

Ritchie, J.T. 1972. Model for predicting evaporation from a row crop with incomplete cover. Water Resour. Res. 8:1204–1213. doi:10.1029/WR008i005p01204

Schwartz, R.C., S.R. Evett, and P.W. Unger. 2003. Soil hydraulic properties of cropland compared with reestablished and native grassland. Geoderma 116:47–60. doi:10.1016/S0016-7061(03)00093-4

Šimůnek, J., M.Th. van Genuchten, and M. Sejna. 2008. Development and applications of the HYDRUS and STANMOD software packages and related codes. Vadose Zone J. 7:587–600. doi:10.2136/vzj2007.0077

Stähli, M., P.-E. Jansson, and L.-C. Lundin. 1996. Preferential water flow in a frozen soil- a two-domain model approach. Hydrol. Processes 10:1305–1316. doi:10.1002/(SICI)1099-1085(199610)10:10<1305::AID-HYP462>3.0.CO;2-F

Stichler, W., G. Eder, E. Stenitzer, and J. Fank. 2005. Isotopenuntersuchungen an den Feldlysimetern und Sickerwassersammlern in Gumpenstein als mögliche Grundlage für Sickerwasserprognosen. *In* Proc. 11. Gumpensteiner Lysimetertagung. 5–6 Apr. 2005. Höhere Bundeslehr- und Forschungsanstalt für Landwirtschaft, A-8952 Irdning.

Stichler, W., and U. Schotterer. 2000. From accumulation to discharge: Modification of stable isotopes during glacial and post-glacial processes. Hydrol. Processes 14:1423–1438. doi:10.1002/1099-1085(20000615)14:8<1423::AID-HYP991>3.0.CO;2-X

Stone, W.W., and J.T. Wilson. 2006. Preferential flow estimates to an agricultural tile drain with implications for Glyphosate transport. J. Environ. Qual. 35:1825–1835. doi:10.2134/jeq2006.0068

Stumpp, C., and P. Maloszewski. 2010. Quantification of preferential flow and flow heterogeneities in an unsaturated soil planted with different crops using the environmental isotope δ^{18}O. J. Hydrol. 394:407–415. doi:10.1016/j.jhydrol.2010.09.014

Stumpp, C., P. Maloszewski, W. Stichler, and J. Fank. 2009a. Environmental isotope (δ^{18}O) and hydrological data to assess water flow in unsaturated soils planted with different crops: Case study lysimeter station "Wagna" (Austria). J. Hydrol. 369:198–208. doi:10.1016/j.jhydrol.2009.02.047

Stumpp, C., P. Maloszewski, W. Stichler, and S. Maciejewski. 2007. Quantification of heterogeneity of the unsaturated zone based on environmental deuterium observed in lysimeter experiments. Hydrol. Sci. J. 52:748–762. doi:10.1623/hysj.52.4.748

Stumpp, C., G. Nützmann, S. Maciejewski, and P. Maloszewski. 2009b. A comparative modeling study of a dual tracer experiment in a large lysimeter under atmospheric conditions. J. Hydrol. 375:566. doi:10.1016/j.jhydrol.2009.07.010

Stumpp, C., W. Stichler, and P. Maloszewski. 2009c. Application of the environmental isotope δ^{18}O to study water flow in unsaturated soils planted with different crops: Case study of a weighable lysimeter from the research field in Neuherberg, Germany. J. Hydrol. 368:68–78. doi:10.1016/j.jhydrol.2009.01.027

van Es, H.M., R.R. Schindelbeck, and W.E. Jokela. 2004. Effect of manure application timing, crop, and soil type on phosphorus leaching. J. Environ. Qual. 33:1070–1080. doi:10.2134/jeq2004.1070

van Es, H.M., J.M. Sogbedji, and R.R. Schindelbeck. 2006. Effect of manure application timing, crop, and soil type on nitrate leaching. J. Environ. Qual. 35:670–679. doi:10.2134/jeq2005.0143

van Genuchten, M.Th. 1980. A closed-form equation for predicting the hydraulic conductivity of unsaturated soils. Soil Sci. Soc. Am. J. 44:892–898. doi:10.2136/sssaj1980.03615995004400050002x

Vanderborght, J., and H. Vereecken. 2007. Review of dispersivities for transport modeling in soils. Vadose Zone J. 6:29–52. doi:10.2136/vzj2006.0096

Vereecken, H., R. Kasteel, J. Vanderborght, and T. Harter. 2007. Upscaling hydraulic properties and soil water flow processes in heterogeneous soils: A review. Vadose Zone J. 6:1–28. doi:10.2136/vzj2006.0055

Vogel, T., M. Cislerova, and J.W. Hopmans. 1991. Porous media with linearly variable hydraulic properties. Water Resour. Res. 27:2735–2741. doi:10.1029/91WR01676

Vogel, T., M. Sanda, J. Dusek, M. Dohnal, and J. Votrubova. 2010. Using oxygen-18 to study the role of preferential flow in the formation of hillslope runoff. Vadose Zone J. 9:252–259. doi:10.2136/vzj2009.0066

Williams, A.G., J.F. Dowd, D. Scholefield, N.M. Holden, and L.K. Deeks. 2003. Preferential flow variability in a well-structured soil. Soil Sci. Soc. Am. J. 67:1272–1281. doi:10.2136/sssaj2003.1272

Zhou, X., H.S. Lin, and E.A. White. 2008. Surface soil hydraulic properties in four soil series under different land uses and their temporal changes. Catena 73:180–188. doi:10.1016/j.catena.2007.09.009

Zimmermann, U., D. Ehhalt, and K.O. Münnich. 1967. Soil-water movement and evapotranspiration: Changes in the isotopic composition of the water. *In* Proc. Isotopes in Hydrology. Proc. Symp., Vienna. IAEA, Vienna, Austria.